Investigation into the effect of plough share leading edge geometry on cable plough performance

Hidetake Matsui[1], S. Robinson[2], M.J. Brown[2], A.J. Brennan[2], C.E. Augarde[3], and W.M. Coombs[3]

[1] Technology Center, Taisei Co., Ltd., 344-1, Nase-cho, Totsuka-ku, Yokohama, 245-0051, Japan.
[2] School of Science and Engineering, University of Dundee, Nethergate, Dundee, DD1 4HN, UK.
[3] Department of Engineering, Durham University, South Road, Durham, DH1 3LE, UK.

ABSTRACT

Cable ploughing is one of the most common means by which subsea cables are buried. Prediction of the cable plough behaviour is important and has the potential to reduce installation costs for offshore renewables. Prediction of tow force and final burial depth is a key factor in choosing appropriate installation equipment and estimating progress rates and the duration of construction. These predictions are currently made using semi-empirical models which create difficulties when attempting to optimise plough designs or predicting plough response in soil conditions which have not previously been experienced. To overcome this issue, the University of Dundee and Durham University, UK are carrying out a project to improve estimation of plough behaviour using small scale physical model testing and Material Point Method numerical analysis. This paper focuses on an effect of plough share leading edge geometry on tow force and final embedment depth based upon small scale model test using model plough shares with different leading edge inclinations. Tests were undertaken in sand at two different relative densities.

Keywords: cable plough; subsea cable; tow force; plough share geometry; offshore wind energy; physical modelling

1 INTRODUCTION

Renewable energy is an important solution to achieve future sustainable human development. Offshore wind energy is one of these renewables and is developing as an alternative energy resource to fossil fuel and nuclear energy. Based upon the increased investment in this technology and the rapid increase in the number of offshore wind farms globally there is a significant need for increased cable installation for interconnection of farms and turbines and transmission back to shore. There are several risks to subsea cables when exposed on the seabed. Impacts from vessels and fishing gear used during trawling as well as snagging from mooring and anchoring can potentially damage cables and lead to costly and lengthy breaks in power transmission (Ivanovic et al 2011).

For protection, subsea cables are typically buried below the seabed surface. A cable plough towed along the seabed by a vessel is a common means by which subsea cables are buried. In the design of cable ploughing, prediction of tow force is critical to choose appropriate equipment and to estimate progress rates of the plough at a certain depth and in a certain soil type. The most commonly used tow force model is that proposed by Cathie (2001) as shown in Eq. (1).

$$F_{cable} = F_w + C_s \gamma D^2 + C_d v\left(C_s \gamma D^2\right) \qquad (1)$$

Where F_w is the force due to the plough self-weight, C_s and C_d are empirical coefficients, γ is the soil unit weight, D is the plough share depth and v is the plough velocity. As shown, there are three terms in this model, each representing the impact of a different variable on the tow force. The first term, F_w, is a function of the plough self-weight and the interface friction ratio of the plough-soil interface. The second term involving C_s accounts for the tow force caused by the static or passive soil resistance. The third term involving C_d accounts for additional tow forces related to the velocity of the plough.

Despite the complexity of plough share geometry and its behaviour, this semi-empirical model takes into account only four parameters, F_w, γ, D and v, related to soil and ploughing conditions. In other words, the empirical coefficients, C_s and C_d, contain a number of other factors affecting tow force such as plough share geometry. In addition, these empirical coefficients are derived from previous field work using existing plough geometries but with potentially limited information on soil conditions due to the sporadic nature of soil sampling or insitu investigation. Therefore, it might be difficult to use this model for optimization of new plough designs or geometry for which there isn't any existing calibration data.

To overcome this issue, the University of Dundee and Durham University are carrying out this project to aid the understanding and estimation of plough behaviour using small scale physical model tests and a new Material Point Method (MPM) analysis (Wang et al, 2017; Cortis et al, 2017). In this project, the effect of

plough share geometry on tow force and plough depth are also being investigated. Robinson et al (2017) investigated the impact of share width on tow forces and improved the prediction model is suggested as shown in Eq. (2).

$$F_{s,cable} = 0.5 C_s^* K_p^2 \gamma W D^2 \quad (2)$$

$$K_p = \frac{1+\sin\phi}{1-\sin\phi} \quad (3)$$

Where C_s^* is a modified empirical coefficient (typically $C_s^* \approx 2$ to 5), K_p is the passive earth pressure coefficient (Eq. (3)), W is the plough share width and ϕ is the critical state friction angle. In the study by Robinson et al (2017), the plough shares were idealized as simple rectangular blocks which were constrained vertically, and dry sand was used for simplicity. Therefore, the force due to the plough self-weight and rate effect were negligible (i.e. Eq. (2) can be compared directly to the second term of Eq. (1)). This model directly accounts for variations in share width for which the existing prediction model has not accounted for directly. This paper focuses on the effect of plough share leading edge inclination angle and reports on 1g small scale model test carried out at the University of Dundee.

2 METHODOLOGIES

2.1 Plough share models

To investigate the effect of plough share inclination angle, a 50th scale cable plough model with three replaceable plough shares with different leading edge inclination were developed (Fig. 1). This allowed for a comparison of tow force and depth during ploughing tests with different plough shares.

2.2 Experimental setup

The apparatus used to perform the ploughing tests is shown in Figure 2. The tests were conducted in a 2.4 m long ploughing tank to ensure that the cable plough models are displaced sufficiently to achieve the steady state (Robinson et al, 2016b). To provide actuation, a DC motor with a variable speed controller was used to move a platform mounted on low friction linear bearings attached to the tank. Tow force was measured by a load cell connected on a rigid vertical frame mounted at the front of platform. Horizontal displacement was measured by a draw wire transducer (DWT) connected to the rear of the platform. For measurement of the position of the cable plough model during ploughing, a linear variable differential transformer (LVDT) measured vertical displacement and a 3-axis MEMs accelerometer measured the pitch and roll of the plough model.

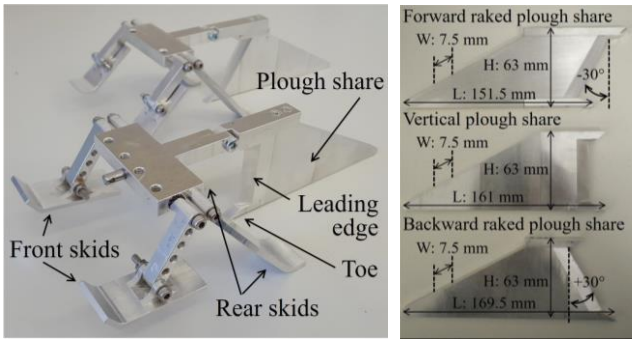

Fig. 1. 1/50th scale cable plough models and plough shares.

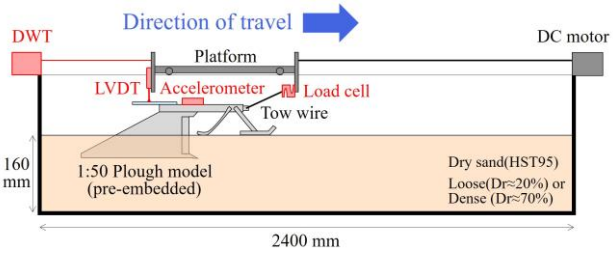

Fig. 2. Schematic of experimental apparatus (the plough shown is not to scale).

Three parameters were varied in the experimental programme to enable their impact on tow forces to be identified; sand relative density, embedment depth and leading edge inclination (Table 1). In addition, as dry sand was used in all tests described in this paper, thus no rate effects occur, meaning that the third term in Eq. (1) is equal to zero.

Table 1. Ranges of parameters used in physical modelling.

Test variables	Sand relative density (%)	Embedment depth (mm)	Leading edge angle (deg.)
Range of parameters used	20 70	10 30 50	-30 0 30

2.3 Material properties

The sand used for the 1g test was uniform fine sand HST95, sourced from Bent Farm in Congleton, Cheshire, UK. The properties of this sand were summarized by Lauder et al (2012), and relevant values are shown in Table 2.

Table 2. Properties of HST95 sand (Lauder et al, 2012).

Property	Value
Maximum dry density, ρ_{max} (kN/m^3)	17.58
Minimum dry density, ρ_{min} (kN/m^3)	14.59
Mean grain diameter, D_{50} (mm)	0.14
Critical state friction angle[1], ϕ'_{crit} (deg.)	32
Critical state interface friction angle[2], δ'_{crit} (deg.)	18

[1] Friction angles determined at normal stresses of 0.2-70 kN/m^3
[2] From tests for this project, not based on Lauder et al (2012).

2.4 Sample preparation

The loose and dense sand beds were prepared by different methods. For preparation of loose sand beds, the sand was placed in a mound at one end of the tank,

and a flat board was used to spread the mound of sand over the length of the box. As the sand was spread, the disturbance allowed consistent loose densities to be achieved. The surface was then scraped to provide a flat surface. The dense sand beds were prepared by dry pluviation using a linear slot pluviator with slot width of 2mm to achieve 70% relative density. The pluviator was moved repeatedly across the ploughing tank at a rate of 150 mm/sec until the required sand bed depth of 160 mm was achieved and then the uneven surface was removed by scraping with a flat edge.

2.5 Test procedure

First, the cable plough model with the plough share was embedded to the required initial depth and attached to the load cell via a tow wire. The draw wire transducer and the DC motor cable were then connected to the platform and a displacement of 1500 mm was applied at a rate of 5 mm/sec by the DC motor whilst logging the various transducers (Fig. 3).

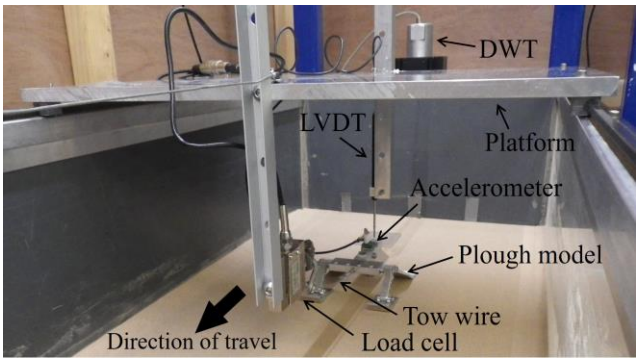

Fig. 3. Cable plough model before test commences.

After the test was complete, the cable plough model was disconnected from the load cell which was removed along with the platform, leaving the cable plough model embedded within the sand bed. This allowed the final undisturbed soil surface to be captured using a 3D scanner and the final surface deformations and trench profiles to be compared with the output from the numerical analysis (by Durham University). The simple low-cost scanning system and its use are described in more detail by Robinson et al (2016a).

3 TEST RESULTS

Figure 4 shows a typical measured tow force during a ploughing test. The data shown relates to the forward raked plough share (-30°), embedded to a depth of 30 mm (1.5 m at prototype scale) in loose sand. As shown, the tow force reaches the steady state rapidly. In subsequent discussion and analysis, average tow forces at the steady state are used for comparison.

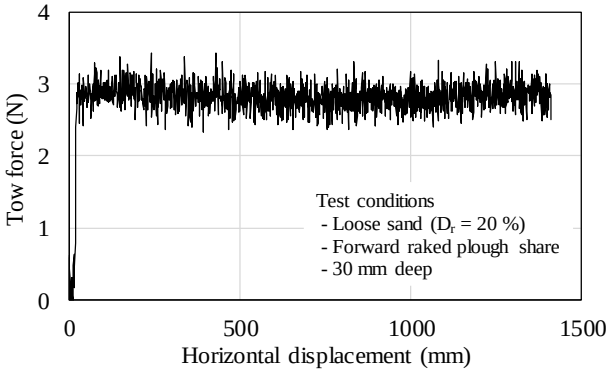

Fig. 4. Typical measured tow force (20% relative density, forward raked plough share and 30mm embedment depth)

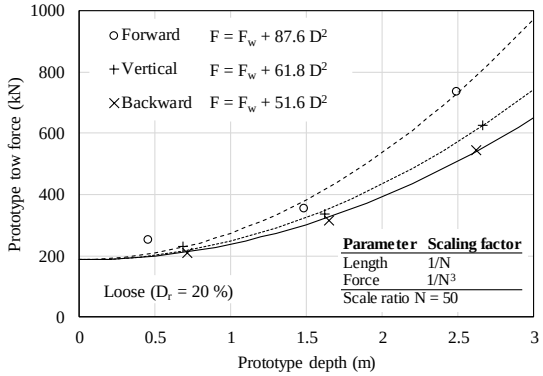

Fig. 5. Tow force against embedment depth for varying plough share leading edge inclination in loose sand (D_r = 20 %).

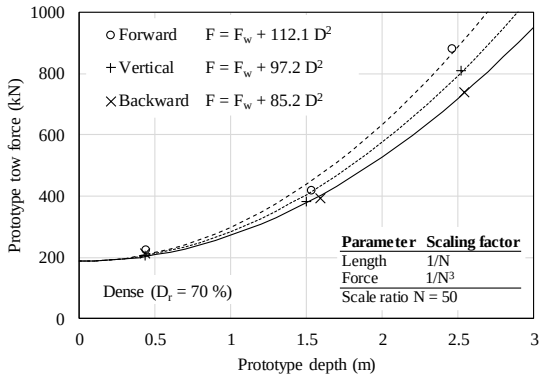

Fig. 6. Tow force against embedment depth for varying plough share leading edge inclination in dense sand (D_r = 70 %).

3.1 Effect of plough share depth

Figure 5 and 6 show the variation of tow force with embedment depth for three plough share leading edge angles at prototype scale. As shown, tow force is affected by the embedment depth as anticipated. The D^2 relationships (derived by least squared fit method) provide a good fit to the measured data points. This validates the form of the existing prediction model proposed by Cathie (2001).

3.2 Effect of plough share leading edge inclination

It is clear that both the tow force and actual final depth is also affected by the plough geometry. The

result for the forward raked plough share (-30°) shows greater tow force in comparison with the vertical plough share (+28% at 2.5m deep in loose sand) and the backward raked plough share (+30°) shows a reduction in tow force. This result seems to be due to the variation of the geometry of the soil wedge (kinematic wedge) in front of the plough share resisting progression of the plough model. This result highlights that a backward plough share might have an advantage in reduction of tow force. It is also noticeable (particularly in loose soil) that the plough tends to reduce in depth with the forward raked share in an attempt to achieve moment equilibrium. This may be accommodated for in practice due to plough skid actuation but it would suggest the plough is less stable in this arrangement.

Figure 7 shows the variation of the empirical coefficient C_s derived from back calculation using the test results and Eq. (1) against plough share leading edge angle. C_s reduces with increasing plough share leading edge angle. A similar tendency is seen in the relationship between passive soil resistance and retaining wall angle known as Coulomb (1776) theory.

Figure 8 shows the variation of the modified empirical coefficient C_s^* derived from back calculation using the test results and Eq. (2) against plough share leading edge angle. A value for C_s^* of 1 would mean

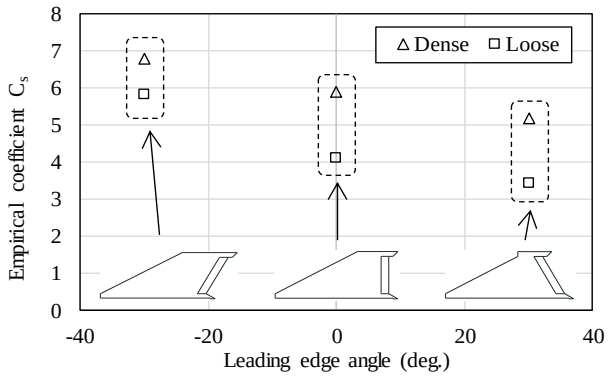

Fig. 7. Empirical coefficient C_s derived from the test against plough share leading edge angle.

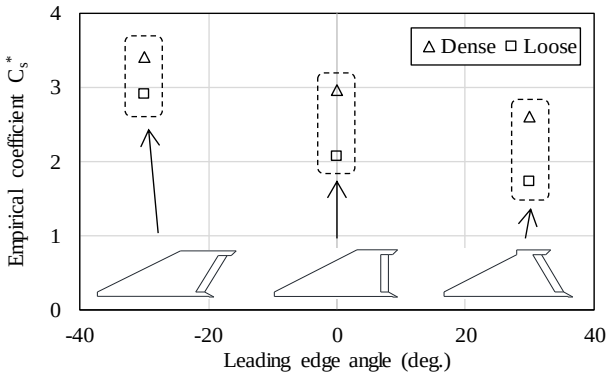

Fig. 8. Modified empirical coefficient C_s^* derived from the test against plough share leading edge angle.

that all aspects of the plough resistance have been accounted for in the model. The fact that the C_s^* values are lower than the values of C_s suggests that using C_s^* is successful in accounting for the plough width, but other factors such as plough side friction still need to be incorporated.

4 CONCLUSIONS

Results from tests using cable plough models with three plough shares with different leading edge inclinations show that both the tow force and actual final depth is affected by the plough geometry and highlight that a backward plough share might have an advantage in reduction of tow force.

ACKNOWLEDGEMENTS

The model seabed ploughing described in this paper has been undertaken as part of the UK EPSRC funded project Seabed ploughing: modelling for infrastructure installation (EP/M000362/1 & EP/M000397/1).

REFERENCES

Cathie, D. (2001). Advances in burial assessment and performance prediction, Int. Cable Protection Committee Plenary Meeting, Tokyo, Japan.

Cortis, M., Coombs, W.M., Augarde, C.E., Robinson, S., Brown, M. and Brennan, A. (2017). Modelling seabed ploughing using the material point method, Proc. of the 1st Int. Conf. on the Material Point Method (MPM 2017), Delft, The Netherlands, 1-7.

Coulomb, C. A. (1776). Essai sur une application des régeles des maximus et minimus a quelque problémes de statique rélatif a l'architecture, Memoirs Divers Savants, 7, Académie Sciences, Paris.

Ivanovic, A., Neilson, R.D. and O'Neill, F.G. (2011). Modelling the physical impact of trawl components on the seabed and comparison with sea trials, Ocean Engineering, Elsevier, 38(7), 925-933.

Lauder, K.D., Brown, M.J., Bransby, M.F. and Boyes, S. (2012). The influence of incorporating a forecutter on the performance of offshore pipeline ploughs, Applied Ocean Research, Elsevier, Vol. 39, 121-130.

Robinson, S., Brown, M.J., Brennan, A.J., Cortis, M., Augarde, C.E. and Coombs, W.M. (2016a). Development of low cost 3D soil surface scanning for physical modelling, Proc. of the 3rd European Conf. on Physical Modelling in Geotechnics (Eurofuge 2016), IFSTTAR, Nantes, France, 159-164.

Robinson, S., Brown, M.J., Brennan, A.J., Cortis, M., Augarde, C.E. and Coombs, W.M. (2016b). Improving seabed cable plough performance for offshore renewable energy, In Guedes Soares (Ed.), Progress in Renewable Energies Offshore, Taylor and Francis, London, 413-419.

Robinson, S., Brown, M.J., Brennan, A.J., Cortis, M., Augarde, C.E. and Coombs, W.M. (2017). Improvement of seabed cable plough tow force prediction models, Proc. 8th Int. conf., Offshore Site Investigation and Geotechnics, Society for Underwater Technology, London, U.K., 914-921.

Wang, L., Coombs, W.M., Augarde, C.E., Brown, M., Knappett, J., Brennan, A., Richards, D. and Blake, A. (2017). Modelling screwpile installation using the MPM, Proc. of the 1st Int. Conf. on the Material Point Method (MPM 2017), Delft, The Netherlands, 124-132.